

# CHARACTERIZATION OF YTTRIA AND MAGNESIA PARTIALLY STABILIZED ZIRCONIA BIOCOMPATIBLE COATINGS DEPOSITED BY PLASMA SPRAYING

RADU ALEXANDRU ROȘU\*, VIOREL-AUREL ȘERBAN\*,  
#ALEXANDRA IOANA BUCUR\*\*, MIHAELA POPESCU\*

\*University "Politehnica" of Timișoara, Faculty of Mechanical Engineering,  
No.1 Mihai Viteazu Blvd., 300222 Timișoara, Romania

\*\*National Institute for Research and Development in Electrochemistry and Condensed Matter Timisoara,  
Analysis and Characterization Dept, no 1 P Andronescu Street, Timisoara 300224, Romania

#E-mail: alexandra.i.bucur@gmail.com

Submitted February 18, 2013; accepted October 1, 2013

**Keywords:** Plasma spraying, Stabilized zirconia, Coatings adherence

*Zirconia ( $ZrO_2$ ) is a biocompatible ceramic material which is successfully used in medicine to cover the metallic implants by various methods. In order to avoid the inconvenients related to structural changes which may appear because of the temperature treatment while depositing the zirconia layer over the metallic implant, certain oxides are added, the most used being  $Y_2O_3$ , MgO and CaO. This paper presents the experimental results regarding the deposition of yttria ( $Y_2O_3$ ) and magnesia (MgO) partially stabilized zirconia layers onto titanium alloy substrate by plasma spraying method. X ray diffraction investigations carried out both on the initial powders and the coatings evidenced the fact that during the thermal spraying process the structure has not been significantly modified, consisting primarily of zirconium oxide with tetragonal structure. Electronic microscopy analyses show that the coatings are dense, uniform and cracks-free. Adherence tests performed on samples whose thickness ranges between 160 and 220  $\mu m$  showed that the highest value (23.5 MPa) was obtained for the coating of  $ZrO_2 - 8 \text{ wt. } \% Y_2O_3$  with 160  $\mu m$  thickness. The roughness values present an increasing tendency with increasing the coatings thickness.*

## INTRODUCTION

Medical implants are, in most of the cases, manufactured from metallic materials because of their good mechanical properties, compared with the ceramic materials [1]. Besides the mechanical properties, the implants must also provide superior biocompatibility, aesthetic and osseointegration properties which sometimes cannot be offered by the metallic materials, the solution being to cover the metal with ceramic materials [2].

The coating layer is very important because it improves the biocompatibility of the metallic substrate by preventing metallic ions releasing and it also improves the acceptance of the implant by the human body, in some cases also having a bactericidal effect [3]. Some of the most used oxide materials in biomedical applications are alumina ( $Al_2O_3$ ) and zirconia ( $ZrO_2$ ) [4].

Pure zirconia exists in three crystallographic phases at different temperatures. At high temperatures ( $> 2370^\circ C$ ) zirconia has a cubic structure. At temperatures between  $1170$  and  $2370^\circ C$  the structure is tetragonal, at temperatures below  $1170^\circ C$ , the structure is mono-

clinic. The tetragonal-monoclinic transformation takes place rapidly and is followed by an increase in volume with 3 - 5 %, which can lead to cracks, decreasing the mechanical properties of the material. In order to remove (reduce) these phenomena (for structure stabilization), some oxides can be added, the most used being  $Y_2O_3$ , MgO and CaO [5].

Wear resistance of zirconia is superior to alumina, the first being used, for instance, for hip prosthesis (cups), where materials with high wear resistance properties are necessary [6].

*In vivo* and *in vitro* studies confirmed the Y-PSZ (Yttria Partially-Stabilized Zirconia) biocompatibility qualities [7], cytotoxicity being similar to alumina. Also, cytotoxic, oncogenic or mutagenic effects of the blood cells or fibroblasts were not observed [8]. *In vivo* behavior of Y-TZP (Yttria Tetragonally-Stabilized Zirconia) showed that no negative reactions of the tissue were developed [9]. Biocompatible tests made on animals show that zirconia implants osseointegration is superior to the osseointegration of those made from titanium alloys [10].

An important problem which often occurs in the case of deposited layers by thermal spraying method is that the coatings can detach from the substrate, leading to implant failure. The coatings adherence plays an important role in thermal spraying processes. The adherence is influenced by many factors like: thermal expansion coefficients (substrate and deposited material), spraying angle, preparation mode of the substrate surface, layers thicknesses [11].

One efficient method which can be used to deposit zirconia on the implants surfaces is plasma spraying, as a result of the high temperatures developed during the spraying processes, temperatures which lead to a melted or plastic state of the powders and achievement of coatings with good adherence [12]. Because of the superior characteristics of the coatings obtained by plasma spraying process, it is the only method approved by Food and Drug Administration (FDA) for medical applications [13]. Also, plasma thermal spraying process is the most appropriate to be used for the deposition of hard ceramic materials owing to the high temperatures developed during the deposition process [14, 20].

The experimental results regarding the deposition of yttria and magnesia partially stabilized zirconia by plasma spraying and the determination of the coatings adherence function of the layers thickness are presented in the paper.

and 220 µm), XRD analysis of the crystalline phases which resulted from the spraying process, SEM analysis of the powder feed and coatings, SEM cross-section images of the deposited layers and adherence determination.

The adherence tests of the coatings were carried out according to the ASTM C633 standard. This method is simple and is often used in industry for determinations of coatings adherence achieved by different thermal spraying methods [15]. In Figure 1 the scheme of the adherence test method according to the ASTM C633 standard is presented.

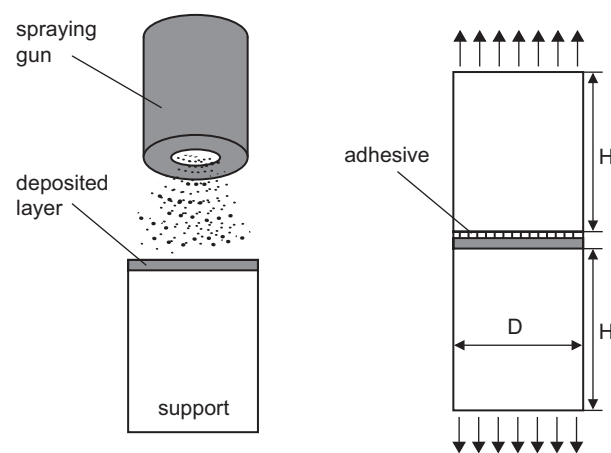


Figure 1. Schematic mode of the adherence test method according to ASTM C633 standard.

## EXPERIMENTAL

### Materials used

The materials used for the experiments were: magnesia partially stabilized zirconia powder ( $ZrO_2$  - 24 wt. % / MgO, Mogul 22) with the particles size between 16 and 63 µm and yttria partially stabilized zirconia powder ( $ZrO_2$  - 8 wt. %  $Y_2O_3$ , Mogul 21) with the dimension of the particles between 12 and 45 µm provided by Mogul Metallizing GmbH. As substrate, titanium alloy (Ti6Al4V) provided by Bibus Steel Company was used.

Before spraying, the titanium substrates were blasted with alumina with the average particle size of 1 mm at the pressure blast of  $6 \cdot 10^5$  Pa and blasting distance of 50 - 60 mm. After blasting, the samples were cleaned with ethylic alcohol.

### Experimental procedure

The experimental procedure consists in the achievement of coatings ( $ZrO_2$  - 24 wt. % / MgO and  $ZrO_2$  - 8 wt. %  $Y_2O_3$ ) with different thicknesses (160, 180, 200

The method consists in bonding the coated sample with an adhesive (cylinder with the diameter of 30 mm) with an uncoated similar sample which was blasted. After that, the samples are tested with a universal testing machine. By tensile test, the value of tensile load which resulted after the separation of the coated-uncoated parts is determined. The adherence value results by calculating the load/area relationship. The failure may occur in the coatings or in the bond coat [16].

### Thermal spraying equipment

Sulzer Metco plasma thermal spraying equipment was used for the deposition of zirconia layers. As plasmagen gas Ar + 6 %  $H_2$  was used, and the carrier gas was argon. The parameters used for the deposition of zirconia coatings by plasma thermal spraying process are presented in Table 1.

Table 1. Parameters used for the deposition of zirconia coatings by plasma thermal spraying.

Plasma Current (A)	Plasma Voltage (V)	Primary Gas Flow (l/min)	Carrier Gas Flow (l/min)	Powder Feed Rate (g/min)	Spray Distance (mm)
550-600	80-90	40-60	10-15	10-15	80-100

Characterization of surface morphology

Scanning electron microscope (SEM) Inspect S with Energy-dispersive X-ray spectroscopy (EDX) was used in order to characterize the surfaces and cross-sections morphology.

The phase composition of the deposited layers was investigated by X-ray diffraction (XRD) using a PANalytical X'Pert Pro MPD diffractometer. The working conditions were 45 kV and 30 mA, using copper radiation with the wavelength  $\lambda = 1.541 \text{ \AA}$ .

The microlayers thickness was determined using an Easy Check F-N device from List-Magnetik and the surface roughness determination was made by using the SurfTest 201 (SJ-201) device from Mitutoyo.

RESULTS AND DISCUSSION

XRD characterization

Figure 2a shows XRD analysis of  $\text{ZrO}_2 - 24 \text{ wt. \%} / \text{MgO}$  powder and Figure 2b presents XRD analysis of  $\text{ZrO}_2 - 24 \text{ wt. \%} / \text{MgO}$  coating obtained by plasma spraying.

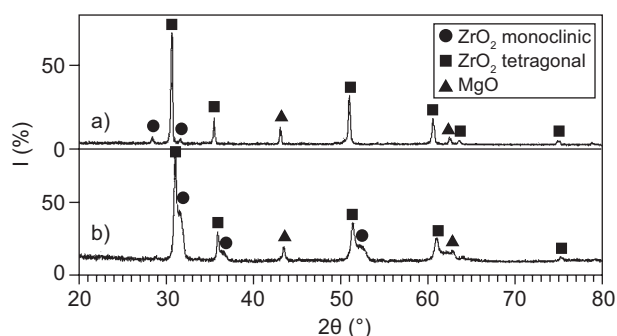


Figure 2. XRD analysis a)  $\text{ZrO}_2 - 24 \text{ wt. \%} / \text{MgO}$  powder, b)  $\text{ZrO}_2 - 24 \text{ wt. \%} / \text{MgO}$  coating.

XRD analysis of  $\text{ZrO}_2 - 24 \text{ wt. \%} / \text{MgO}$  coating deposited by plasma spraying shows that the structure is composed of  $\text{ZrO}_2$  with tetragonal and monoclinic structure and magnesium oxide (MgO). These crystallographic phases, present in the initial powders (as seen in Figure 2), are also present in the achieved deposited layer; while the tetragonal phase is relatively stable in behavior, the monoclinic phase presents an increase in intensity and number of peaks. This behavior explains the pattern shift to the right, meaning a potential thermal stress, induced in the coating by the existence of a slightly higher amount of monoclinic phase (the volume of the tetragonal elementary cell is lower compared with the volume of monoclinic elementary cell). Unfortunately, a quantification of the concentration of the two phases was not possible. The XRD results show that the structure did not suffer important modifications in terms of composition during the spraying process.

Figure 3a shows the XRD analysis of Y-PSZ (Yttria Partially-Stabilized Zirconia) powder and Figure 3b presents the XRD results of the coatings obtained by plasma spraying.

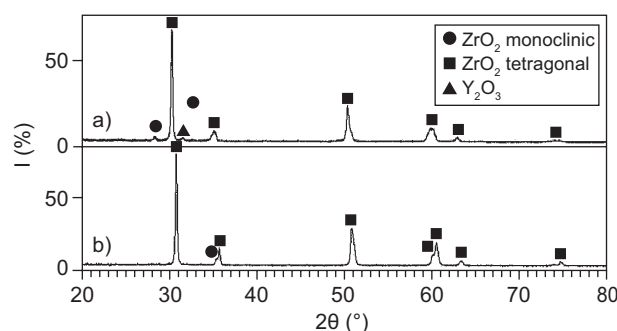


Figure 3. XRD analysis: a)  $\text{ZrO}_2 - 8 \text{ wt. \%} \text{ Y}_2\text{O}_3$  powder; b)  $\text{ZrO}_2 - 8 \text{ wt. \%} \text{ Y}_2\text{O}_3$  coating.

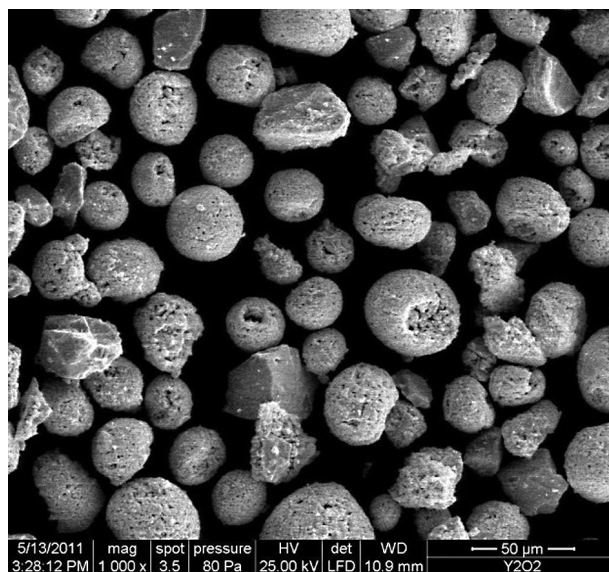
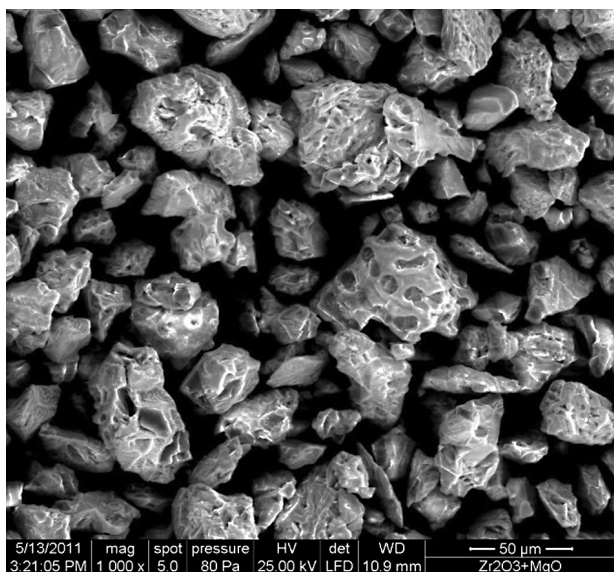


Figure 4. SEM image of  $\text{ZrO}_2 - 24 \text{ wt. \%} \text{ MgO}$  and  $\text{ZrO}_2 - 8 \text{ wt. \%} \text{ Y}_2\text{O}_3$  powders before deposition.



XRD analysis of  $ZrO_2 - 8 \text{ wt. } \% Y_2O_3$  powder shows that the structure is composed of  $ZrO_2$  with tetragonal structure,  $ZrO_2$  with monoclinic structure and yttria oxide ( $Y_2O_3$ ); it can be observed that the coatings did not present important modifications during the spraying process.

In both cases it can be noticed that the peaks are shifted to the right for the deposited layers, indicating a thermal stress of the sample because of the thermal treatment they were subjected to. Also, a small number of peaks disappear and new peaks appear after the deposition process, explainable by the  $ZrO_2$  changes in crystalline phases.

#### SEM analysis of the powders

Figure 4 presents the morphology of  $ZrO_2 - 24 \text{ wt. } \% MgO$  and  $ZrO_2 - 8 \text{ wt. } \% Y_2O_3$  powders used for deposition.

SEM analysis shows that the particles have an irregular shape in the case of  $ZrO_2 - 24 \text{ wt. } \% MgO$  and spherical shape for the case of  $ZrO_2 - 8 \text{ wt. } \% Y_2O_3$  powder. The size of these particles lies in the range  $16 - 63 \mu m$ . The surface of the particles is rather rough, in both cases, property which is considered to be a plus in achieving good adhesion properties.

#### The microstructure of the $ZrO_2$ coatings

Figure 5 presents the SEM images of  $ZrO_2 - 24 \text{ wt. } \% MgO$  coatings and Figure 6 presents the SEM images of  $ZrO_2 - 8 \text{ wt. } \% Y_2O_3$  coatings obtained by plasma spraying.

The cross sections SEM images of the both previously mentioned layers deposited by plasma spraying are presented in Figures 7 and 8. These show that the particles melted during the spraying process and depo-

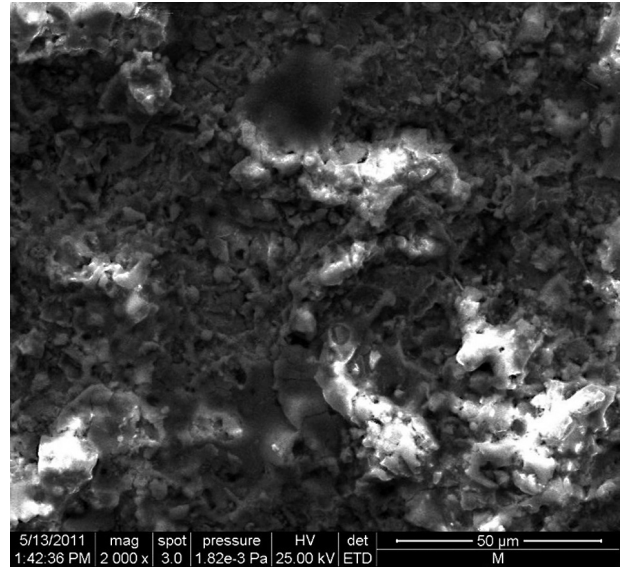
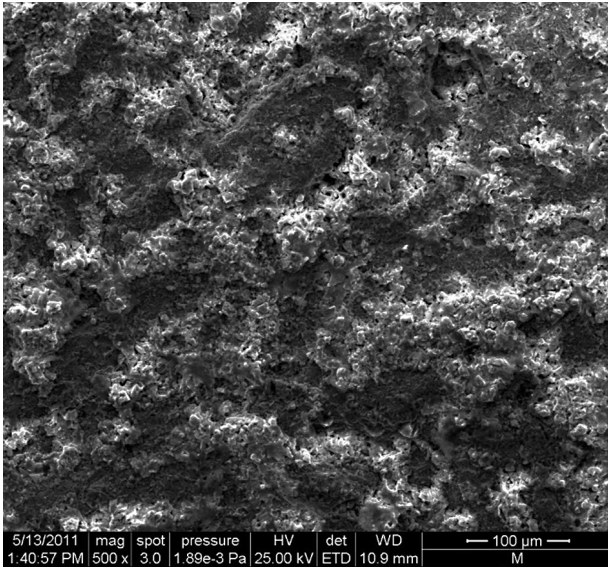


Figure 5. SEM images of  $ZrO_2 - 24 \text{ wt. } \% MgO$  coatings obtained by plasma spraying.

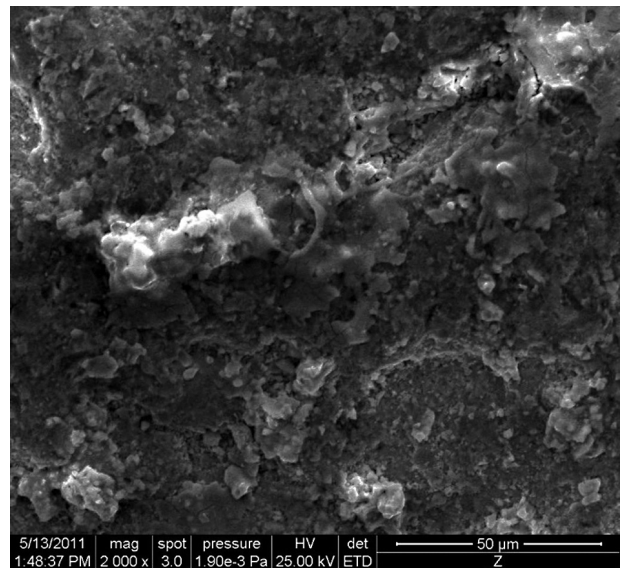
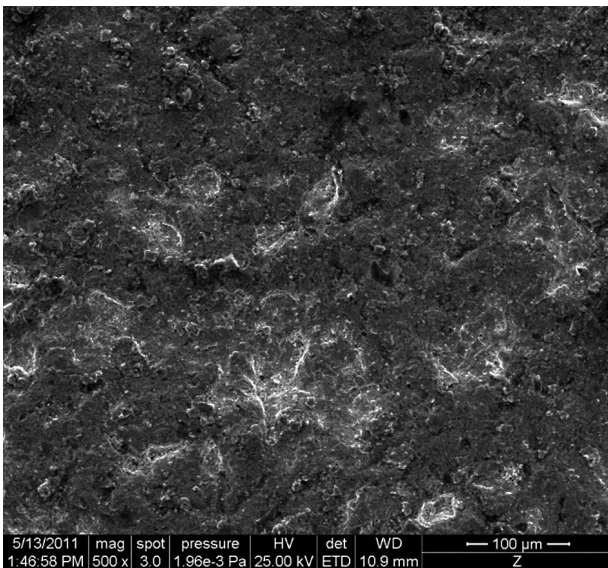


Figure 6. SEM images of  $ZrO_2 - 8 \text{ wt. } \% Y_2O_3$  coatings obtained by plasma spraying.

sited onto the titanium alloy led to the formation of compact and slightly rough coatings.

The cross section of the both zirconia coatings ( $ZrO_2 - 24 \text{ wt. \% MgO}$  and  $ZrO_2 - 8 \text{ wt. \% Y}_2O_3$ ) reveal that the coatings have the typical morphology of the plasma sprayed coatings, containing pores. It can also be seen that the  $ZrO_2 - 8 \text{ wt. \% Y}_2O_3$  coating is denser than  $ZrO_2 - 24 \text{ wt. \% MgO}$  coating, which can lead to a better adherence.

#### Determination of coatings roughness and thickness

The coatings made by plasma spraying using the two zirconia powders ( $ZrO_2 - 8 \text{ wt. \% Y}_2O_3$  and  $ZrO_2 - 24 \text{ wt. \% MgO}$ ) have thickness values which range between 160 and 220  $\mu\text{m}$ , measured with Easy Check device, and roughness values between 4.01 and 5.03  $\mu\text{m}$  (measured with F-N Surftest 201). Table 2 presents the

thickness and roughness values of the coatings deposited by plasma spraying.

It can be observed that the thickness of the coatings influences the surfaces roughness in both types of samples; it can be seen that the roughness values increase by increasing the coatings thickness, a phenomenon also observed by other authors in their research on ceramic coatings made by plasma spraying [17].

#### Adhesion of coatings

Failure of the deposited layers adhesion is based on various factors which include microcracks owing to different thermal expansion coefficients of the coating-substrate materials. These cracks will be responsible for changes in mechanical properties (especially hardness). Moreover, in some cases an oxide layer is formed between the deposited layer and adhesive, layer that has different thicknesses which depend on the oxidation

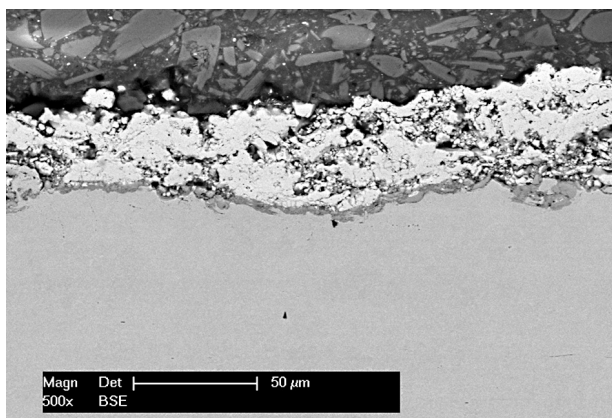


Figure 7. Cross section of  $ZrO_2 - 24 \text{ wt. \% MgO}$  coatings.

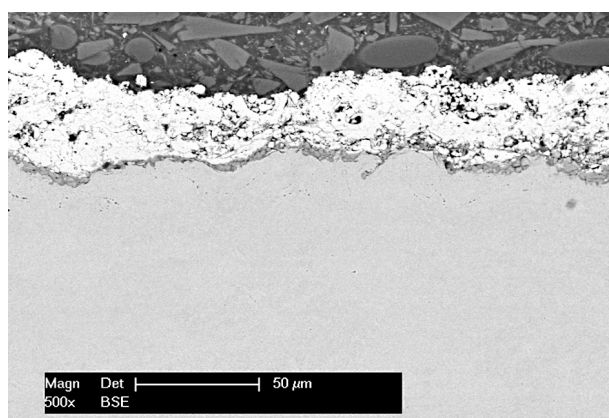


Figure 8. Cross section of  $ZrO_2 - 8 \text{ wt. \% Y}_2O_3$  coatings.

Table 2. Roughness and thickness values of zirconia coatings deposited by plasma spraying.

Sample	Coating thickness ( $\mu\text{m}$ )	Roughness ( $\mu\text{m}$ )	
		$ZrO_2 - 24 \text{ wt. \% MgO}$ coatings	$ZrO_2 - 8 \text{ wt. \% Y}_2O_3$ coatings
1	$160 \pm 15$	4.01	4.25
2	$180 \pm 15$	4.31	4.79
3	$200 \pm 15$	4.47	4.93
4	$220 \pm 20$	4.80	5.03

Table 3. Adherence values depending on the coating thickness.

$ZrO_2 - 24 \text{ wt. \% MgO}$ coatings			
Sample	Coating thickness ( $\mu\text{m}$ )	Adherence value (MPa)	Breaking mode
1	$160 \pm 15$	20.7	Bond coat/ceramic interface
2	$180 \pm 15$	19.1	Bond coat/ceramic interface
3	$200 \pm 15$	18.6	Bond coat/ceramic interface
4	$220 \pm 20$	18.1	Bond coat/ceramic interface
$ZrO_2 - 8 \text{ wt. \% Y}_2O_3$ coatings			
Sample	Coating thickness ( $\mu\text{m}$ )	Adherence value (MPa)	Breaking mode
1	$160 \pm 15$	23.5	Glue
2	$180 \pm 15$	23.1	Glue
3	$200 \pm 15$	22.4	Bond coat/ceramic interface
4	$220 \pm 20$	22.6	Bond coat/ceramic interface



kinetics [18, 19]. These oxide layers can lead to an increase in hardness of the deposited layer, but have a negative effect on coatings adherence. Table 3 presents the adherence values depending on the coating thickness, resulted after the adherence test according to ASTM C-633.

The fractographs of the specimens after the adherence test for both coatings ( $ZrO_2 - 24 \text{ wt. \% MgO}$  and  $ZrO_2 - 8 \text{ wt. \% Y}_2O_3$ ) are presented in figures 9 and 10.

The left side of the figures shows the coated surface and the right side shows the glued surface. It can be noticed that in both coatings, the breaking occurred in the ceramic interface, except for two coatings of  $ZrO_2 - 8 \text{ wt. \% Y}_2O_3$  (at thickness of  $160 \mu\text{m}$  and  $180 \mu\text{m}$ ) where the breaking occurred in the adhesive layer. It is also observable that in both cases the coatings adherence

increases with the decreasing of the coatings thickness reaching the maximum value of  $23.5 \text{ MPa}$  for  $ZrO_2 - 8 \text{ wt. \% Y}_2O_3$  coating with the thickness of  $160 \mu\text{m}$ , where the breaking occurred in the adhesive layer. It was also observed that  $ZrO_2 - 24 \text{ wt. \% MgO}$  coatings present slightly lower values compared with  $ZrO_2 - 8 \text{ wt. \% Y}_2O_3$  coatings as a result of their higher porosity.

As a result of the performed work, we can conclude that the deposition method we have chosen for  $ZrO_2 - 24 \text{ wt. \% MgO}$  and  $ZrO_2 - 8 \text{ wt. \% Y}_2O_3$  powders is proper for biomaterials because it does not alter the substrate or the coating structure, as could be seen from XRD and SEM analysis, thus preserving their mechanical properties. Depending on the desired application, the mechanical characteristics of the coated implant can be modeled (according to a conducted

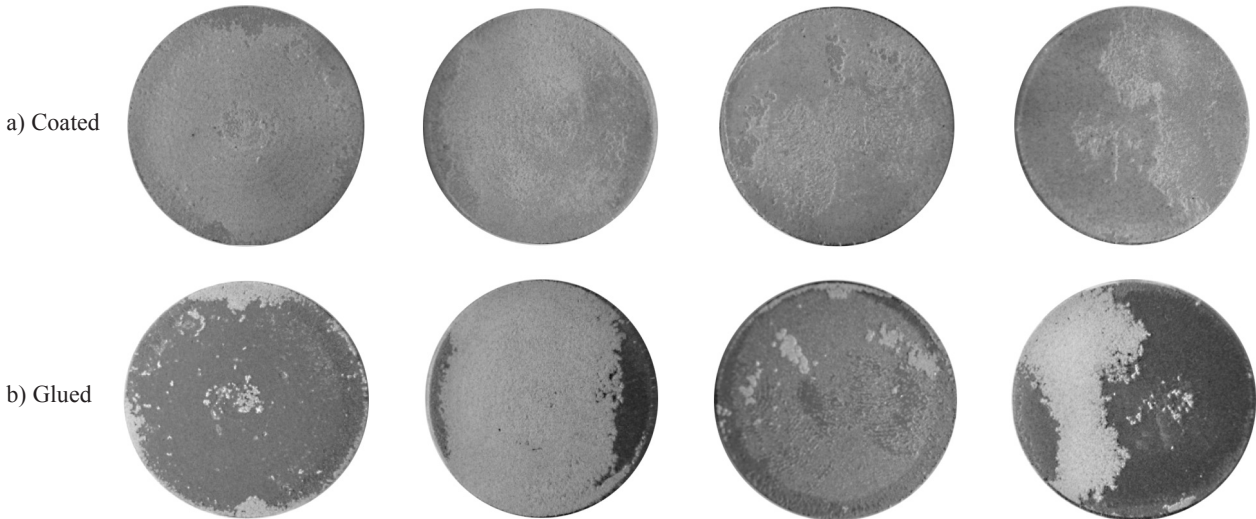


Figure 9. Fractographs of  $ZrO_2 - 24 \text{ wt. \% MgO}$  coatings at the four mentioned thicknesses increasing from top to bottom after the adherence test.

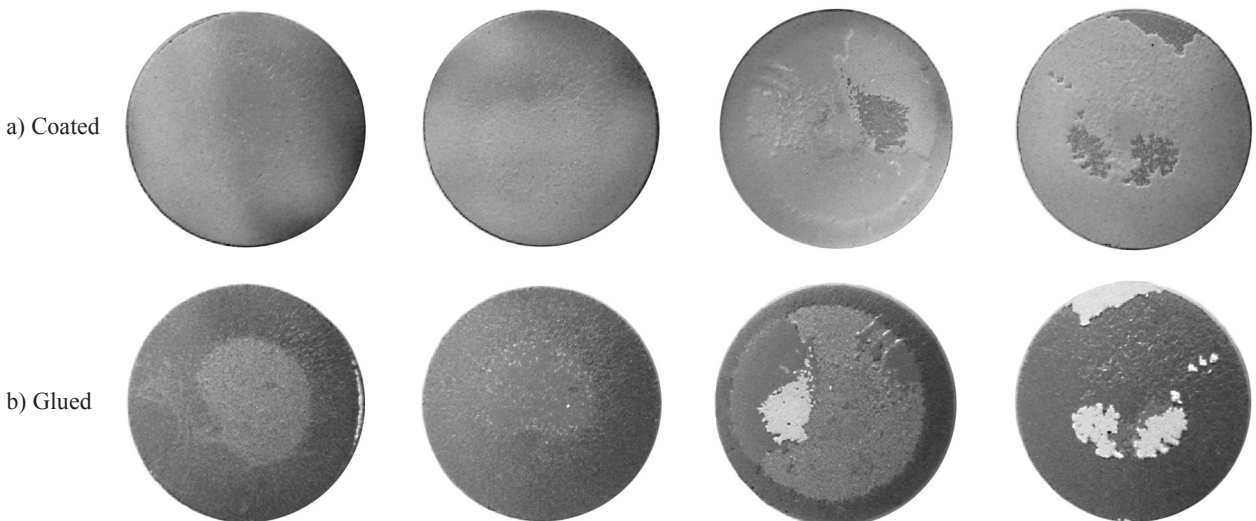


Figure 10. Fractographs of  $ZrO_2 - 8 \text{ wt. \% Y}_2O_3$  coatings at the four mentioned thicknesses increasing from top to bottom after the adherence test.

study) in order to obtain the maximum performance. The physico-chemical characteristics determined in this study recommend these coatings for biomedical tests in vitro and in vivo.

For future research activity we will try to study the deposition and evaluation of biocomposite coatings consisting of zirconia stabilized with different oxides in combination with hydroxyapatite. In this way we hope to improve the biocompatibility and bioactivity of the coatings, results which will hopefully be confirmed by the tests in Simulated Body Fluid (SBF).

### CONCLUSIONS

- Coatings of ZrO<sub>2</sub> - 24 wt. % MgO and ZrO<sub>2</sub> - 8 wt. % Y<sub>2</sub>O<sub>3</sub> mixture powders were obtained by plasma thermal spraying at four different spraying distances; the deposited layers were physico-chemically analyzed by XRD and SEM and tests were conducted in order to determine the roughness and adhesion of the coatings onto the Ti substrate.
- X-ray diffraction of zirconia coatings (ZrO<sub>2</sub> - 24 wt. % MgO, respectively ZrO<sub>2</sub> - 8 wt. % Y<sub>2</sub>O<sub>3</sub>) showed that during the thermal spraying process significant structure changes were not produced; the structure is mainly composed of ZrO<sub>2</sub> with tetragonal and monoclinic structure and oxides: yttrium oxide (Y<sub>2</sub>O<sub>3</sub>) and magnesium oxide (MgO) respectively
- Deposited zirconia coatings analysis showed that they are dense, compact and defects-free (such as exfoliations or cracks)
- Adherence tests taken in accordance with ASTM C633 standard showed that the highest adhesion values were obtained for ZrO<sub>2</sub> - 8 wt. % Y<sub>2</sub>O<sub>3</sub> coatings (23.5 MPa), where the break occurred in the adhesive layer, compared with ZrO<sub>2</sub> - 24 wt. % MgO coatings where the break occurred in the bond coat/ceramic interface. It is also observable that the thickness of the deposited layers influences the surface roughness in both types of zirconia.

### Acknowledgement

*This work was partially supported by the strategic grant POSDRU/89/1.5/S/57649, Project ID 57649 (PER-*

*FORM-ERA), co-financed by the European Social Fund – Investing in People, within the Sectorial Operational Programme Human Resources Development 2007-2013. Special thanks to Prof. Dr.-Ing. Waltraut Brandl and Dr.-Ing. Gabriela Marginean from Westfälische Hochschule Gelsenkirchen, Germany for their very valuable help.*

### REFERENCES

1. Nasab M. B., Hassan M. R.: Trends. Biomater. Artif. Organs 24, 69 (2010).
2. Heimann R. B.: CMU 1, 23 (2002).
3. Tirrell M., Kokkoli E., Biegalski M.: Surf. Sci. 500, 61 (2002).
4. Denry I., Holloway J. A.: Materials 3, 351 (2010).
5. Piconi C., Maccauro G.: Biomaterials 20, 25 (1999).
6. Kumar P., Oka M., Ikeuchi K., Shimizu K., Yamamuro T., Okumura H., Koloura Y., J. Biomed. Mater. Res. 25, 813 (1991).
7. Thamaraiselvi T. V., Rajeswari S.: Trends Biomater. Artif. Organs 18, 9 (2004).
8. Vagkopoulou T., Koutayas S. O., Koidis P., Strub J. R. : Eur. J. Esthet. Dent. 4, 130 (2009).
9. Piconi C., Burger W., Richter H.G., Cittadini A., Maccauro G., Covacci V., Bruzzese N., Ricci G.A., Marmo E.: Biomaterials 19, 1489 (1998).
10. Manicone P. F., Iommetti P. R., Raffaelli L.: J. Dent. 35, 819 (2007).
11. Bahbou M.F., Nysten P., Wigren J.: J. Therm. Spray Technol. 13, 508 (2004).
12. Kulkarni A., Golland A., Herman H., Allen A. J., Ilavsky J., Long G., Carlo F.: J. Therm. Spray Technol. 14, 239 (2005).
13. Singh G., Singh S., Prakash S.: J. Miner. & Mat. Charact. & Eng. 9, 1059 (2010).
14. Rosu R. A., Serban V. A., Bucur A. I., Dragos U.: Appl. Surf. Sci. 258, 3871 (2012).
15. Vilotijevic M., Markovic P., Zec S., Marinkovic S., Jokanovic V.: J. Mat. Process. Technol. 211, 996 (2011).
16. Lima C.R.C., Guilemany J.M.: Surf. Coat. Technol. 201, 4694 (2007).
17. Ozkan Sarikaya: Surf. Coat. Technol. 190, 388 (2005).
18. Schlichting K.W., Pature N.P., Jordan E.H., Gell M.: Mat. Sci. Eng. A 342, 120 (2003).
19. Teixeira V., Andritschky M., Gruhn H., Malléner W., Buchkremer H.P., Stöver D.: J. Therm. Spray Technol. 9, 191 (2000).
20. Serban V. A., Rosu R. A., Bucur A. I., Pascu D. R.: Appl. Surf. Sci. 265, 245 (2013)..